THE JOURNAL OF BIOLOGICAL CHEMISTRY VOL. 288, NO. 7, pp. 5007–5016, February 15, 2013

In Vivo Regulation of Steroid Hormones by the Chst10 Sulfotransferase in Mouse*[S]

Received for publication, November 5, 2012, and in revised form, December 23, 2012 Published, JBC Papers in Press, December 26, 2012, DOI 10.1074/jbc.M112.433474

Misa Suzuki-Anekoji[‡], Atsushi Suzuki[‡1], Sz-Wei Wu[§], Kiyohiko Angata[‡2], Keith K. Murai[‡3], Kazuhiro Sugihara[¶], Tomoya O. Akama[‖], Kay-Hooi Khoo[§], Jun Nakayama[**], Michiko N. Fukuda[‡4], and Minoru Fukuda[‡5]

*From the [‡]Glycobiology Unit, Tumor Microenvironment Program, Cancer Center, Sanford-Burnham Medical Research Institute, La Jolla, California 92037, the [§]Institute of Biological Chemistry, Academia Sinica, Taipei 11529, Taiwan, the [¶]Department of Gynecology and Obstetrics, Hamamatsu University School of Medicine, Hamamatsu 431-3192, Japan, the [‖]Department of Pharmacology, Kansai Medical University, Osaka 570-8506, Japan, and the **Department of Molecular Pathology, Shinshu University Graduate School of Medicine, Matsumoto 390-8621, Japan*

Background: Chst10 transfers sulfate to glucuronic acid to form the HNK-1 antigen carried by glycoproteins and glycolipids in neurons and NK cells.
Results: Chst10 transfers sulfate to glucuronidated steroid hormones, and *Chst10*-deficient mice exhibited subfertility.
Conclusion: Subfertility in *Chst10* null females is caused by a loss of steroid hormone dysregulation.
Significance: This study identified a new regulatory mechanism mediated by sulfation of glucuronidated steroid.

Chst10 adds sulfate to glucuronic acid to form a carbohydrate antigen, HNK-1, in glycoproteins and glycolipids. To determine the role of Chst10 *in vivo*, we generated systemic *Chst10*-deficient mutant mice. Although *Chst10*$^{-/-}$ mice were born and grew to adulthood with no gross defects, they were subfertile. Uteri from *Chst10*$^{-/-}$ females at the pro-estrus stage were larger than those from wild-type females and exhibited a thick uterine endometrium. Serum estrogen levels in *Chst10*$^{-/-}$ females were higher than those from wild-type females, suggesting impaired down-regulation of estrogen. Because steroid hormones are often conjugated to glucuronic acid, we hypothesized that Chst10 sulfates glucuronidated steroid hormone to regulate steroid hormone *in vivo*. Enzymatic activity assays and structural analysis of Chst10 products by HPLC and mass spectrometry revealed that Chst10 indeed sulfates glucuronidated estrogen, testosterone, and other steroid hormones. We also identified an HPLC peak corresponding to sulfated and glucuronidated estradiol in serum from wild-type but not from *Chst10* null female mice. Estrogen-response element reporter assays revealed that Chst10-modified estrogen likely did not bind to its receptor. These results suggest that subfertility exhibited by female mice following Chst10 loss results from dysregulation of estrogen. Given that Chst10 transfers sulfates to several steroid hormones, Chst10 likely functions in widespread regulation of steroid hormones *in vivo*.

Sulfated glycans play diverse roles in development, differentiation, and homeostasis. These glycans provide a ligand for lymphocytes homing to lymph nodes (1–9) or blastocysts rolling on endometrial epithelia (10–12), alter binding of growth factors to receptors (13), function in the clearance of circulating glycoprotein hormones (13, 14), participate in formation of a transparent cornea (15), and play critical roles in embryonic development of species as diverse as mice (16) and *Drosophila* (17).

Monoclonal antibodies specifically recognizing sulfated glycan epitopes have served as useful reagents for defining cellular activities mediated by sulfated glycans (5, 18–23). The monoclonal antibody HNK-1, which was raised against human natural killer cells (24), recognizes a unique glycan structure terminated by sulfated glucuronic acid linked to *N*-acetyl-lactosamine or SO_3→3GlcUAβ1→3Galβ1→4GlcNAcβ1→R (18). The HNK-1 epitope is carried by both glycoproteins and glycolipids (18, 25–31). This antigen has also been found in neuronal cells (32, 33). HNK-1 antigen found on adhesion molecules such as neural cell adhesion molecule (32, 33), MAG (34), L2 (35), P0 (36), GluR2 (37), RPTPβ (38), and CD24 (39) is suggested to modulate adhesion of HNK-1-positive cell types (35). Neurite outgrowth by mouse motor neurons is facilitated by an HNK-1 glycolipid substratum (40). However, neurite outgrowth on neural cell adhesion molecule is inhibited by HNK-1 glycan (41). These findings suggest that HNK-1 glycan plays a regulatory role in neuronal cell-cell/matrix interaction.

To synthesize the HNK-1 epitope, mammalian cells require two enzymes, B3GAT1 (or β1,3-glucuronyltransferase) (42) and CHST10 (or HNK-1 sulfotransferase) (43, 44). Previously,

* This work was supported, in whole or in part, by National Institutes of Health Grants P01CA071932 (to M. N. F. and M. F.), EY014620 (to T. O. A.), and CA33895 (to M. F.). This work was also supported by Japanese Ministry of Education Grant 24592530 (to A. S.).
⌘ *Author's Choice*—Final version full access.
[S] This article contains supplemental Figs. S1–S7.
[1] Present address: Dept. of Gynecology and Obstetrics, Keio University School of Medicine, Tokyo 160-8582, Japan.
[2] Present address: National Institute of Advanced Industrial Science and Technology, Tsukuba, Ibaragi 305-8586, Japan.
[3] Present address: Center for Research in Neuroscience, Research Institute of the McGill University Health Center, Montreal General Hospital, Montreal, Quebec H3G 1A4, Canada.
[4] To whom correspondence may be addressed: Tumor Microenvironment Program, Cancer Center, Sanford-Burnham Medical Research Institute, 10901 N. Torrey Pines Rd., La Jolla, CA 92037. Tel.: 858-646-3143; E-mail: michiko@sanfordburnham.org.
[5] To whom correspondence may be addressed: Tumor Microenvironment Program, Cancer Center, Sanford-Burnham Medical Research Institute, 10901 N. Torrey Pines Rd., La Jolla, CA 92037. Tel.: 858-646-3144; E-mail: minoru@sanfordburnham.org.

we found that CHST10 contains a conserved RDP sequence in the 3′-phosphoadenosine phosphosulfate (PAPS)[6] binding domain (44). CHST10 also shares a 5′-PAPS binding domain with cytosolic sulfotransferases, such as the estrogen sulfotransferase Sult1E1 (45, 46). *Sult1E1*-deficient female mice are reportedly infertile due to a placental defect and exhibit spontaneous loss of embryos (47, 48).

Steroid hormones, including estrogen, are synthesized from cholesterol in the ovary and testis via coordinated activities of enzymes such as cytochrome P450s, 17β-hydroxysteroid dehydrogenases, and aromatase (49). In liver, some steroid hormones are conjugated with glucuronic acid by uridine-diphosphoglucuronic acid transferases (UGTs). UGT family proteins, encoded by *UGT1* and *UGT2* genes (50), consist of more than 15 enzymes formed by alternative splicing of transcripts of these genes. Glucuronidation of steroid hormones blocks their binding to corresponding receptors, down-regulating bioactive hormones *in vivo*. Glucuronidation also converts steroid hormones into more water-soluble products, facilitating removal from the circulation. In addition to glucuronidation, sulfation also plays a role in down-regulating steroid hormones (51).

To investigate the *in vivo* role of Chst10, we generated systemic *Chst10*-deficient mice. *Chst10* null mice grew to adulthood without exhibiting gross abnormalities. However, *Chst10* null mice bred infrequently and had a small litter size. We used these mice to determine whether Chst10 transfers sulfate to glucuronidated steroid hormones, with a focus on sulfation of glucuronidated estrogen. Those genetic studies, combined with biochemical approaches, suggest that Chst10 regulates estrogen *in vivo* in the female mouse.

MATERIALS AND METHODS

Generation of Chst10-deficient Mice—A *Chst10* targeting vector was constructed as shown in Fig. 1. Homologously recombined ES clones were selected by Southern hybridization using a probe adjacent to the targeting vector. Probe DNA (about 450 bp) was amplified by PCR using the following primers: 5–12s, TGTAGTCAAGGCAGCAACCAAGCA, and 5–13a, GAGCGCCAAACAGCAGCAG. Genomic DNA was digested with EcoRI to distinguish the targeted (3.8 kb) from the wild-type (7.4 kb) allele. To assess whether the line is maintained, genotyping was performed by PCR using the following primers: 5–3 (5′-primer in Neo), GTGCTACTTCCATTGTCACG; 5–10 (3′-primer in the common sequence), TCTTTCAGTCGAGGATGGTGGCA; and 5–11 (5′-primer in deleted sequence), GCTGCTTGTGAAATCGGGTACTTG.

Blood Steroid Hormone Levels—The estrus cycle of female mice was determined by vaginal smears following a standard procedure (52). Blood from female mice was collected in the mornings at the pro-estrus stage, and serum was separated and stored at −80 °C. Quantitative analysis of mouse blood steroid hormones was carried out by radioimmunoassay at the Ligand Assay and Analysis Core Facility of University of Virginia Center for Research in Reproduction.

In Vitro Sulfation and Glycosylation of Steroids—Sulfation of GlcUA steroids *in vitro* by recombinant Chst10 was performed as described (44). The reaction mixture (100 μl) contained 0.9 nmol (3 μCi) of [^{35}S]PAPS, 2 mM unlabeled PAPS, 100 mM Tris-HCl, pH 7.2, 0.1% Triton X-100, 10 mM $MnCl_2$, 2.5 mM ATP, and 3 mM acceptor glucuronidated steroid. A recombinant protein A-conjugated soluble form of CHST10 was produced in COS cells. A protein A-CHST10 chimera collected from culture supernatants was purified and concentrated to ~50 times by CentriPrep YM-10 (Millipore). Purified enzyme was added in the reaction mixture. After incubation at 37 °C for 20–60 min, ice-cold ethanol (500 μl) was added to stop the reaction. The ethanol-soluble fraction was collected and concentrated using a SpeedVac. Steroids were purified using a 0.2-ml bed volume solid phase extraction column (High Load C_{18}; Alltech). The sample was dissolved in 0.25 M ammonium formate, pH 4.0, applied to the column, and washed with the same buffer. Sulfated steroids were eluted in 70% methanol and then concentrated and subjected to HPLC analysis described below.

Glucuronidation of steroid *in vitro* was performed in a manner similar to that described above. The reaction mixture contained the following: 50 μM Tris-HCl, pH 7.5, 10 mM $MgCl_2$, 0.1 mg/ml phosphatidylcholine, 8.5 mM D-saccharic acid α1,4-lactone, 15 mM (3 μCi) of [^{3}H]UDP-GlcUA, 0.5 mM unlabeled UDP-GlcUA, and acceptor steroid. The reaction mixture was incubated at 37 °C for 16 h, and the reaction product was purified using High Load C_{18} solid phase extraction column described above and then subjected to HPLC analysis. The enzyme source was either recombinant UGT or a mouse liver microsome fraction, prepared as described (53).

HPLC Analysis—GlcUA- and/or SO_3-GlcUA-modified steroids were analyzed by HPLC using an Ascentis C_{18} reverse phase column (4.6 mm × 15 cm, 5-μm particles) (SUPELCO). Solvent A was composed of 90% 5 mM tetrabutyl ammonium sulfate in water, 7.5% acetonitrile and 2.5% methanol. Solvent B was composed of 30% 5 mM tetrabutyl ammonium sulfate, 52% acetonitrile, and 17.5% methanol. Unmodified and modified steroid hormones were separated using the following elution programs. Program 1, 100% A for 10 min followed by a gradient up to 100% B over 40 min, followed by 100% B over 15 min. The flow rate was 1 ml/min. Program 2 is the same as program 1, except the initial elution with A is for 12 min. Elution positions of standard steroids (50 nmol) were monitored by absorbance at 220 nm. Radiolabeled GlcUA- or SO_3-GlcUA-modified steroids were collected every minute, and radioactivity was measured by a scintillation counter.

Preparation of SO_3-GlcUA-3-E_2—The Chst10 reaction mixture (100 μl) was identical to that described above without radiolabeled PAPS (44, 45). Product SO_3-GlcUA-3-E_2 was purified twice by HPLC using either an Ascentis C_{18} column, as described above for mass spectrometry, or Zorbax SB-C18 (Agilent). A 4.6 mm × 25 cm column was programmed to be washed by a linear gradient of 30% buffer B (75% acetonitrile in methanol) in 70% buffer A (5 mM tetrabutyl ammonium sulfate-H_2O) up to 10 min followed by a gradient to 60% B over 30 min,

[6] The abbreviations used are: PAPS, phosphoadenosine phosphosulfate; GlcUA, glucuronic acid; LacNAc, *N*-acetyllactosamine; E_2, 17-β-estradiol; ER, estrogen receptor; ERE, estrogen-responsive element; UGT, uridine-diphosphoglucuronic acid transferase.

followed by 100% B over 5 min. The flow rate was 1 ml/min. Elution of SO_3-GlcUA-E_2 was monitored by UV absorbance at 220 nm. Purified SO_3-GlcUA-3-E_2 was used for estrogen receptor reporter assay.

Digestion of Steroid Conjugates by Glycosidases—HPLC analysis of glycosidase-digested samples was performed as follows. The radiolabeled steroid fraction was desalted using a High Load C_{18} solid phase extraction column and dried in a tube under a SpeedVac. *Escherichia coli*-derived β-glucuronidase (Sigma) (1 μl) was added to the steroid fraction dissolved in 20 μl of 50 mM Tris-HCl, pH 6.8, and incubated at 37 °C for 16 h. Aryl sulfatase from *Helix pomatia* (Sigma) (1 μl) was added to the steroid fraction dissolved in 20 μl of 50 mM Tris-HCl, pH 6.5, plus 8.5 mM D-saccharic acid α1,4-lactone incubated at 37 °C for 1 h.

Mass Spectrometry Analysis—The samples were dissolved in 50% (v/v) acetonitrile in water and injected into a Q-TOF Ultima API mass spectrometer (Micromass) by direct infusion or by static nanospray. Both MS and MS/MS data were acquired in negative ion mode. For direct infusion, the flow rate was set as 0.3 μl/min, and the spray voltage was set as 3.5 kV. Nanoflow Probe Tip (M956231AD1-S, Waters™) was used for static nanospray, and the spray voltage was set as 900 V. All spectra were interpreted manually.

Estrogen-responsive Element (ERE) Gene Activation Assay—HEK293T cells were cultured in a 10-cm plate using phenol red-free DMEM containing 5% charcoal/dextran-treated FBS. Cells were transfected with the pBIND-ERα (Promega) expression vector, which contains the yeast Gal4 DNA binding domain and an estrogen receptor-ligand binding domain gene fusion that can induce the transcription of luciferase gene in the pGL4.35 vector when activated by a ligand.

Three hours after transfection, cells were seeded at 1×10^5 cells/well in 96-well tissue culture plates. One day later or on the 2nd day of transfection, cells were treated with serial dilutions of ligands, including E_2. Then 24 h after ligand stimulation, luciferin was added to the culture medium at 0.6 mg/ml, and chemiluminescence was measured in a Beckman DTX880 plate reader.

RESULTS

Targeted Disruption of Chst10 in the Mouse—Targeting disruption of *Chst10* for systemic gene knock-out was performed using methods similar to those described previously (54). Because the RDP sequence found in the Chst10 catalytic domain (45) is encoded by exon 5, we disrupted exon 5 by homologous recombination (Fig. 1*A*). Two lines of ES cells harboring homologous recombinant clones were identified by Southern hybridization using probes adjacent to the targeting vector (Fig. 1*B*), and those cells were injected into blastocysts to generate mutant mice. Elimination of HNK-1 antigen in *Chst10* null mice was confirmed by immunohistochemistry of brain tissue using anti-HNK-1 antibody (Fig. 1*C*).

Breeding of Chst10-deficient Mutant Mice—Neither male nor female *Chst10*$^{-/-}$ mice showed gross morphological anomalies in brain tissues (supplemental Fig. S1). However, both male and female *Chst10*$^{-/-}$ mice were subfertile, and crosses between *Chst10*$^{+/-}$ males and females yielded pups at the rate of 8.11/litter ($n = 17$); those between wild-type and *Chst10*$^{-/-}$ often did not produce pups or produced pups at a low rate of 5.4/litter ($n = 5$, statistical significance with $p = 0.005$ by unpaired two-tailed Student's *t* test) (supplemental Fig. S2). These observations suggest that Chst10 functions in male and female reproduction.

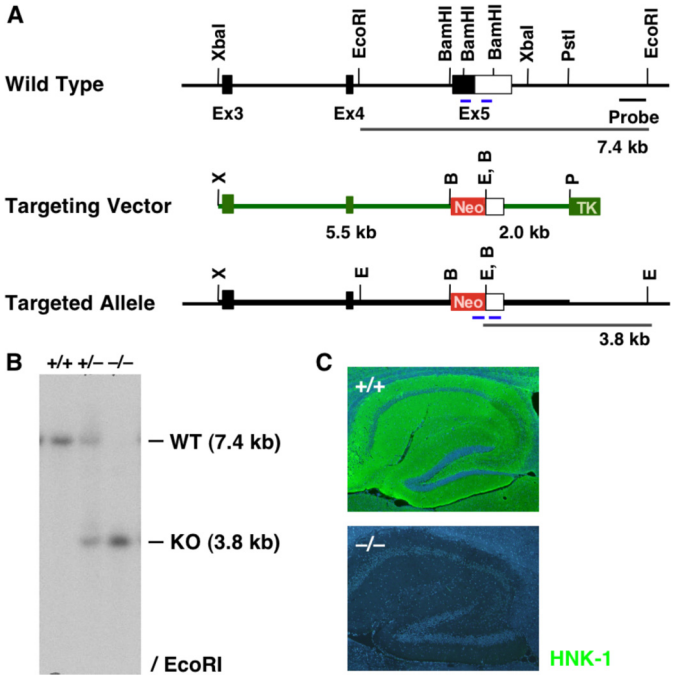

FIGURE 1. **Targeting of the *Chst10* gene.** *A*, targeting of the *Chst10* gene. *A, Chst10* was ablated by replacing exon 5 encoding the catalytic domain with PGK-Neo (*Neo*). XbaI-BamHI (5.5 kb) and BamHI-PstI (2.0 kb) fragments were subcloned into the targeting vector for homologous recombination. *B,* Southern hybridization. Genomic DNA was digested with EcoRI, and DNA fragments separated on agarose gels were transferred to a membrane, which was hybridized to a labeled probe denoted by a *black bar* in *A*. *C,* immunostaining of the mouse hippocampus by an anti-HNK-1 antibody. HNK-1 antigen is highly expressed in the hippocampus of wild-type but not in *Chst10*-deficient mouse brain, confirming that Chst10 is the sole sulfotransferase that generates HNK-1 antigen. Nuclei are stained with Hoechst 33342 (*blue*).

Abnormalities in Female Reproductive Organs of Chst10$^{-/-}$ *Mice*—To assess a potential role for *Chst10* in reproduction, we focused on female *Chst10*$^{-/-}$ mice. Analysis of morphology of female reproductive organs revealed that uteri of *Chst10*$^{-/-}$ females from the pro-estrus phase were larger than those from *Chst10*$^{+/+}$ females (Fig. 2, *A, upper panel* and *B*). Sections of uterine tissue showed that the endometrium was thicker in *Chst10*$^{-/-}$ compared with *Chst10*$^{+/+}$ mice (Fig. 2*A, lower panel*). Because growth of endometrial epithelia requires E_2, this observation suggested that E_2 is more active in *Chst10*$^{-/-}$ than in Chst10$^{+/+}$ mice. Indeed, serum E_2 levels in *Chst10*$^{-/-}$ females at pro-estrus stages were higher than those seen in *Chst10*$^{+/+}$ mice (Fig. 2*C*), suggesting that E_2 down-regulation is impaired in the former. As anticipated, the hormonal cycle of uteri of *Chst10*$^{+/+}$ females was regular, whereas that of *Chst10*$^{-/-}$ females showed signs of disruption (supplemental Fig. S3).

Chst10 Transfers Sulfate to Glucuronidated Sex Steroid Hormones—Steroid hormones are reportedly glucuronidated in liver as an excretion mechanism *in vivo* (51). Because glu-

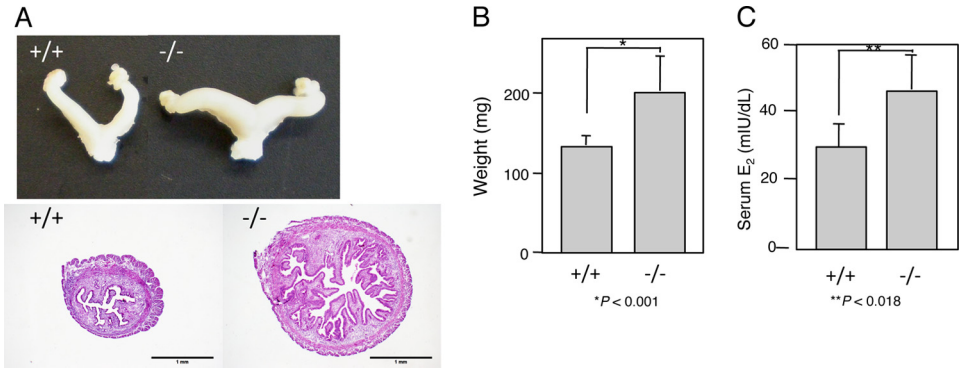

FIGURE 2. **Abnormalities *in uteri* from *Chst10*-deficient mutant female mice.** *A*, *Chst10*$^{-/-}$ mice show enlarged uteri compared with wild-type mice based on histology and organ weight. Note extensive growth of endometrial epithelial layers in hematoxylin and eosin-stained uterine sections from *Chst10*$^{-/-}$ compared with *Chst10*$^{+/+}$ females. *B*, average weight of uteri from *Chst10*$^{+/+}$ ($n = 10$) and *Chst10*$^{-/-}$ ($n = 4$). *C*, estrogen levels in sera from *Chst10*$^{+/+}$ ($n = 4$) and *Chst10*$^{-/-}$ ($n = 3$) females at the pro-estrus stage. *B* and *C*, Student's *t* test was used for statistical analysis.

curonide is a Chst10 substrate, we asked whether Chst10 transfers sulfate to glucuronidated steroid hormones (Fig. 3 and supplemental Fig. S4). *In vitro* analysis indicated that various glucuronidated steroids serve as good acceptor substrates for Chst10. These findings suggest that Chst10 prefers GlcUA at the 3-hydroxyl group of a sterol ring over 17-hydroxyl (Fig. 3, *3rd* and *4th columns*). Among the steroids tested, GlcUA-3-androstane (5β-androstane-3α,17-α-diol-11-one-17-β carboxylic acid 3-β-D-glucuronide), an androgen variant, appeared to be the best acceptor substrate, followed by GlcUA-3-E_2 (17-β-estradiol-3-GlcUA), a major form of estrogen. Dehydroepiandrosterone-3-GlcUA and GlcUA-17-testosterone (testosterone-17-GlcUA) also served as Chst10 acceptors (Fig. 3 and supplemental Fig. S5). Chst10 did not transfer sulfate to substrates lacking glucuronic acid (Fig. 3).

The kinetics of Chst10 relative to representative acceptor substrates was determined using radioactive [^{35}S]PAPS as a donor. A reaction mixture of [^{35}S]PAPS and GlcUA-3-E_2 yielded a single peak in HPLC for SO_3-GlcUA-3-E_2 (Fig. 4*A*, *lower panel*). Kinetic analysis (Fig. 5 and Table 1) suggested that GlcUA-3-E_2 is a 3-fold better Chst10 substrate than is GlcUAβ1–3LacNAc, the precursor of HNK-1 antigen. These results suggest strongly that Chst10 may transfer sulfate to the glucuronidated steroid hormones *in vivo*.

To confirm structures of sulfated glucuronidated steroid hormone products, SO_3-GlcUA-3-E_2 was prepared by incubating GlcUA-E_2 with nonradiolabeled PAPS and recombinant Chst10, and products were purified by HPLC (Fig. 4*A*, *upper panel*). Elution position of SO_3-GlcUA-3-E_2 was ascertained by assessing elution positions of radiolabeled peaks (Fig. 4*A*, *lower panel*). Based on nanoESI-MS/MS analyses, this product afforded the expected $[M - H]^-$ molecular ion signal at *m/z* 527.22 in negative ion mode for SO_3-GlcUA-3-E_2. Further MS/MS analysis suggested common loss of the sulfate moiety (−80 *m/z*) and yielded the set of fragment ions at *m/z* 97, 175, and 255, corresponding to HSO_4^-, $GlcUA^-$, and SO_3-GlcUA, respectively (Fig. 4*B*). This analysis indicated that the product carried the expected terminally sulfated GlcUA substituent.

We synthesized SO_3-GlcUA-E_2 *in vitro* by transferring [^{3}H]GlcUA from [^{3}H]UDP-GlcUA using a recombinant protein A-UGT1A1 fusion protein. The reaction product analyzed by HPLC showed two peaks, most likely GlcUA-3-E_2 and GlcUA-17-E_2, based on elution positions of authentic GlcUA-3-E_2 and GlcUA-17-E_2 (supplemental Fig. S6, *upper panel*). We reacted both peaks with [^{35}S]PAPS and soluble recombinant Chst10, which resulted in disappearance of the two GlcUA-E_2 peaks and the appearance of a [^{35}S]SO_3-[^{3}H]GlcUA peak (supplemental Fig. S6, *lower panel*). Because both SO_3-GlcUA-3-E_2 and SO_3-GlcUA-17-E_2 were eluted at the same position in prior experiments (Fig. 4*A*), we conclude that the ^{35}S- and ^{3}H-double-labeled product peak represents a mixture of SO_3-GlcUA-3-E_2 and SO_3-GlcUA-17-E_2. These observations indicate that two recombinant enzymes, UGT1A1 and Chst10, can be used to synthesize glucuronidated and sulfated E_2 *in vitro*.

Detection of SO_3-GlcUA-E_2 in Mouse Serum—To detect SO_3-GlcUA-E_2 *in vivo* in the mouse, female mice were injected intravenously with either [^{3}H]E_2 or [^{35}S]SO_3 (inorganic sulfate). Serum was collected 24 h after injection, and radioactive products were analyzed by HPLC (Fig. 6). In Chst10$^{+/+}$ mice, [^{3}H]E_2 was converted to several compounds (Fig. 6*A*, *upper panel*). The one that eluted at 42 min matches the elution position of E_2, which was a prominent peak in Chst10$^{-/-}$ serum (Fig. 6*A*, *lower panel*). A peak seen at 46 min in Chst10$^{+/+}$ mice matched the elution position of SO_3-GlcUA-3-E_2 (Fig. 6, *A* and *B*, *upper panels, shown by arrows*). This peak was not detected in samples from Chst10$^{-/-}$ mice (Fig. 6, *A* and *B*, *lower panels*).

Products derived from [^{3}H]E_2-injected *Chst10*$^{+/+}$ were subjected to sulfatase and β-glucuronidase digestion (Fig. 6*C*). Digestion of products by β-glucuronidase dismissed peaks at 28, 31, 34, and 38 min (Fig. 6*C*, *panels a* and *b*), suggesting that these compounds are capped by glucuronic acids. However, arylsulfatase digestion of [^{3}H]E_2 products dismissed peaks at 31, 36, 38, and 46 min, suggesting that these compounds are sulfated at the terminus (Fig. 6*C*, *panels a* and *c*). The 46-min peak, presumably representing SO_3-GlcUA-3-E_2, was shifted to GlcUA-3-E_2 at 28 or 34 min after arylsulfatase digestion, indicating that sulfate was at the terminus of this compound and shifted to GlcUA-3-E_2 (Fig. 6*C*, *panel c*). Digestion of ^{3}H-labeled products with a mixture of β-glucuronidase and arylsulfatase dismissed all peaks except E_2 at 42 min (Fig. 6*C*, *panel d*), suggesting that all metabolites detected by HPLC in Fig. 6*C*, *panel a*, are glucuronidated and/or sulfated E_2.

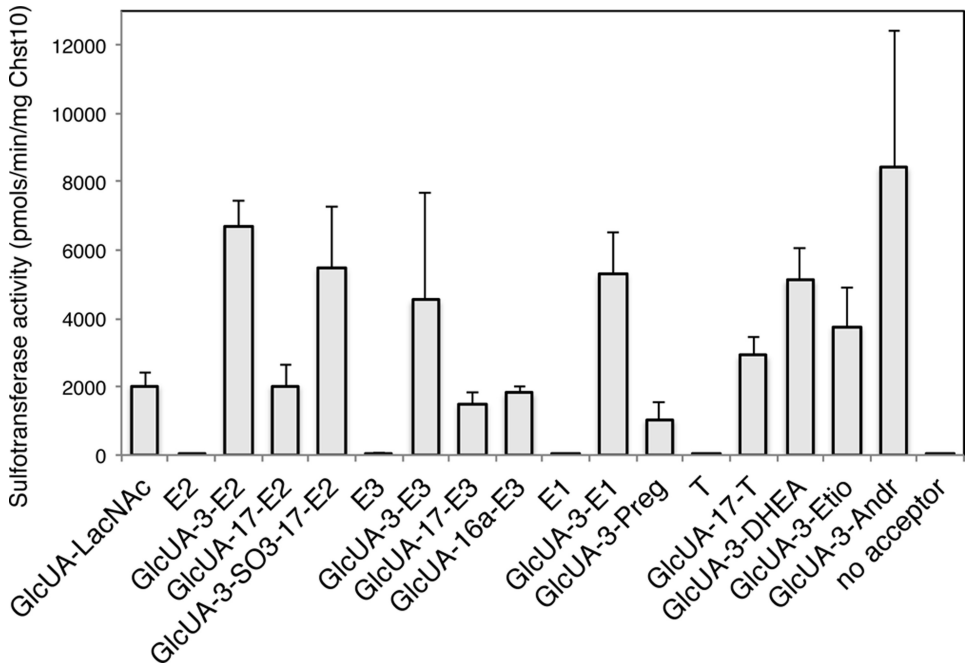

FIGURE 3. **Chst10 sulfate-transferring activity toward various steroid hormones.** [^{35}S]PAPS was incubated with each steroid plus Chst10, and the yield of sulfated product was determined. Structures of each substrate are shown in supplemental Fig. S4. Each measurement was done as a duplicate. *Error bars* represent standard deviation.

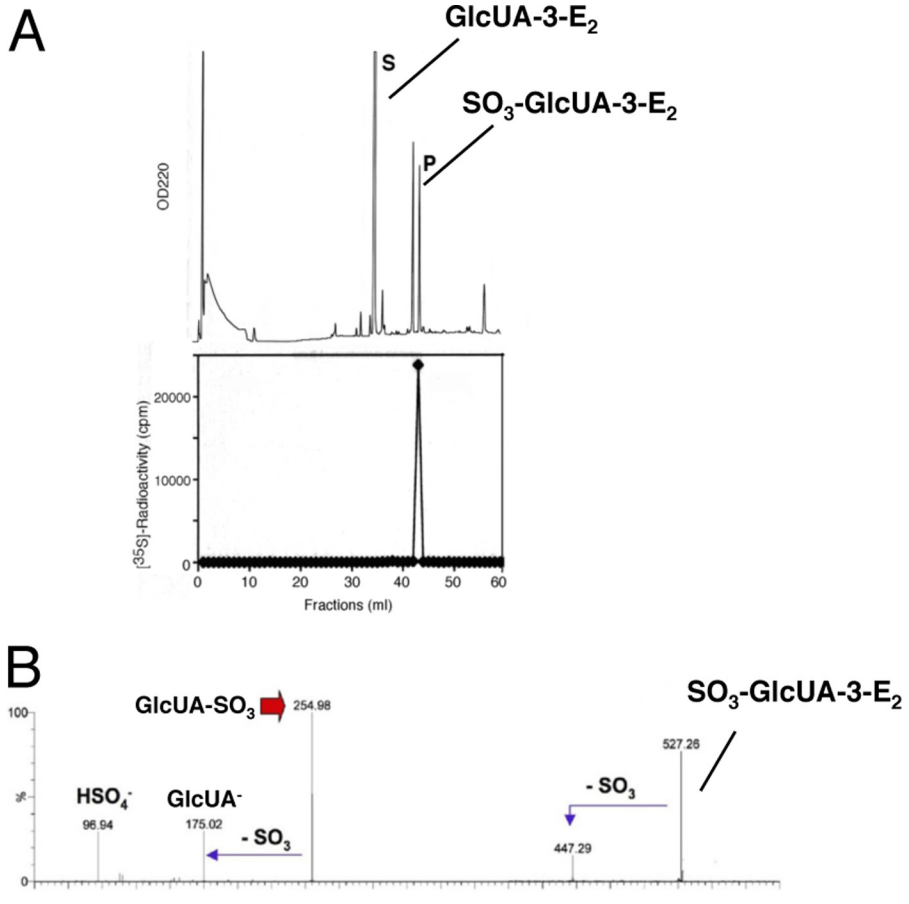

FIGURE 4. **HPLC and mass spectrometry analysis of sulfated GlcUA-E_2 *in vitro*.** *A*, GlcUA-3-E_2 was incubated with Chst10 and [^{35}S]PAPS, and radioactive product was analyzed by HPLC using program 1 (see "Materials and Methods"). A prominent peak at 43 min matches the elution position of SO_3-GlcUA-E_2 (*A*, *lower panel*). A large peak in front of peak *P* is likely unmodified E_2, as authentic E_2 elutes at this position under the HPLC conditions used in this experiment (data not shown). *B,* product was isolated and subjected to nanoESI-MS and MS/MS analysis. SO_3-GlcUA-E_2 afforded the expected $[M - H]^-$ molecular ions at *m/z* 527. This ion was further subjected to MS/MS, and the major product ions observed were assigned as annotated.

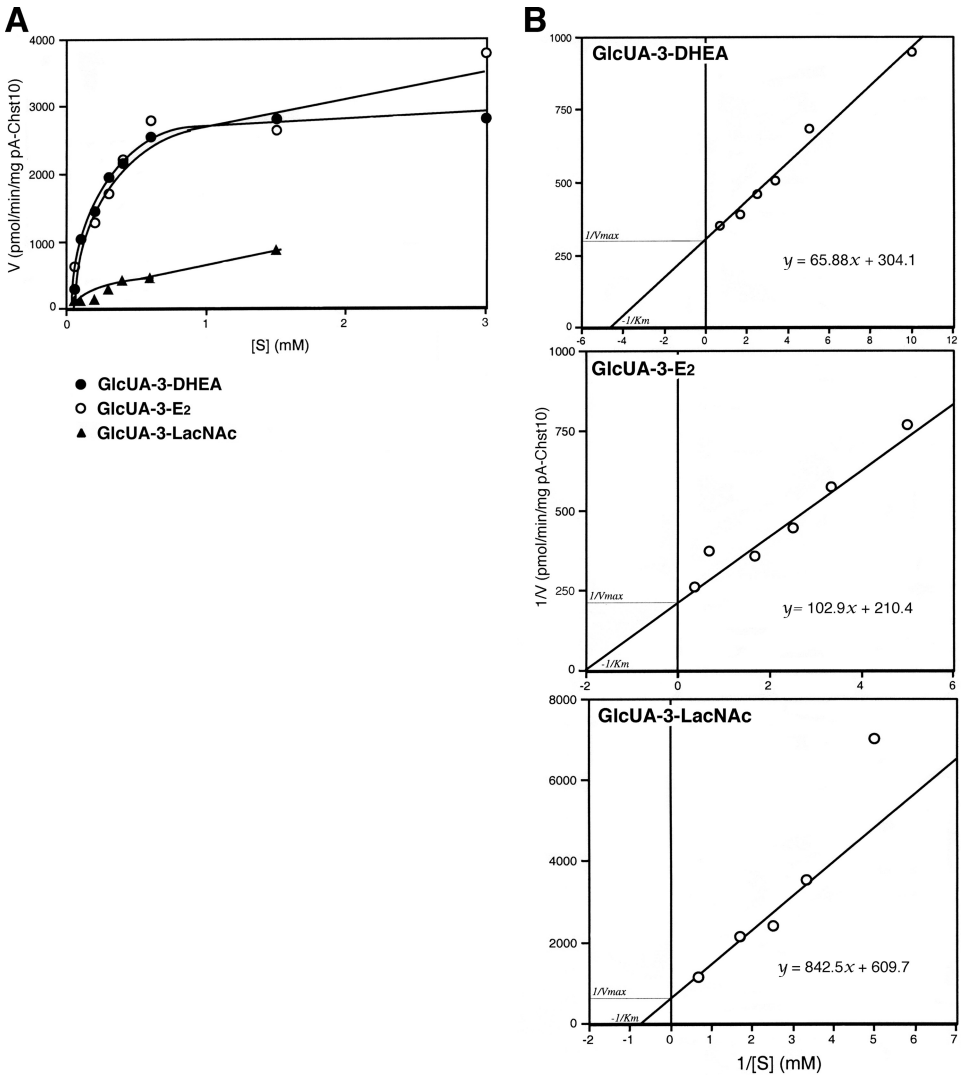

FIGURE 5. **Kinetics analysis of Chst10.** *A,* Chst10 activity dependence on acceptor concentration of GlcUA-3-dehydroepiandrosterone (*DHEA*), GlcUA-3-E_2, and GlcUA-LacNAc substrates. *B,* Michaelis-Menten plots of GlcUA-3-dehydroepiandrosterone A (*top panel*), GlcUA-3-E_2 (*middle panel*), and GlcUA-LacNAc (*bottom panel*).

TABLE 1

Kinetic properties of Chst10 activity toward three acceptors: GlcUA-3-DHEA, GlcUA-3-E_2, and GlcUA-LacNAc

DHEA is dehydroepiandrosterone.

Acceptor	K_m (mM) ± S.E.	V_{MAX}
		pmol/min/mg Chst10
GlcUA-3-DHEA	0.210 ± 0.035	3194 ± 157
GlcUA-3-E_2	0.321 ± 0.081	3858 ± 329
GlcUA-3-LacNAc	1.518 ± 0.464	1723 ± 331

When $[^3H]E_2$ was injected intravenously into a *Chst10*$^{-/-}$ mouse, $[^3H]E_2$ was not all converted into those seen in wild-type (Fig. 6*A*, *lower panel*). When $[^{35}S]SO_4$ was injected into the Chst10$^{+/+}$ mouse, several ^{35}S-labeled peaks, including SO_3-GlcUA-3-E_2 (Fig. 6*B*, *upper panel, shown by an arrow*), appeared. By contrast, those major ^{35}S-labeled peaks found in Chst10$^{+/+}$ mice were not detected in Chst10$^{-/-}$ (Fig. 6*B*, *lower panel*), suggesting that peaks shown in Fig. 6*B, upper panel* are sulfated E_2 derivatives.

Homing of SO_3-GlcUA-E_2 in Vivo in the Mouse—To gain insight into SO_3-GlcUA-3-E_2 function, we performed a homing assay in the mouse. $[^3H]E_2$ was injected intravenously into female mice, and 3 h later radioactivity in representative organs was determined. Significant radioactivity was recovered in the uterus and liver (supplemental Fig. S7), consistent with the idea that E_2 goes to organs where ERs are expressed at high levels (55). When ^{35}S-labeled or $[^3H]SO_3$-GlcUA-3-E_2 was used in this assay, SO_3-GlcUA-3-E_2 was recovered largely from urine, from digested materials in small intestines, and from serum (supplemental Fig. S7), suggesting that SO_3-GlcUA-E_2 is excreted from the body through the entero-hepatic pathway.

SO_3-GlcUA-3-E_2 Activity in Cells Expressing ERs—SO_3-GlcUA-3-E_2 activity relevant to ERs was verified by luciferase-based promoter assays employing an ERE (Fig. 7). Luciferase and ER vectors were co-transfected into ER-negative HEK293T cells, and cells were then treated with E_2, GlcUA-3-E_2, SO_3-3-E_2, or SO_3-GlcUA-3-E_2. Cells co-transfected with ER and luciferase reporter constructs showed luciferase activity when treated with 10^{-8} M E_2. By contrast, neither GlcUA-3-E_2 nor SO_3-GlcUA-3-E_2 promoted this activity at concentrations as high as 10^{-6} M, indicating that they are relatively poor activa-

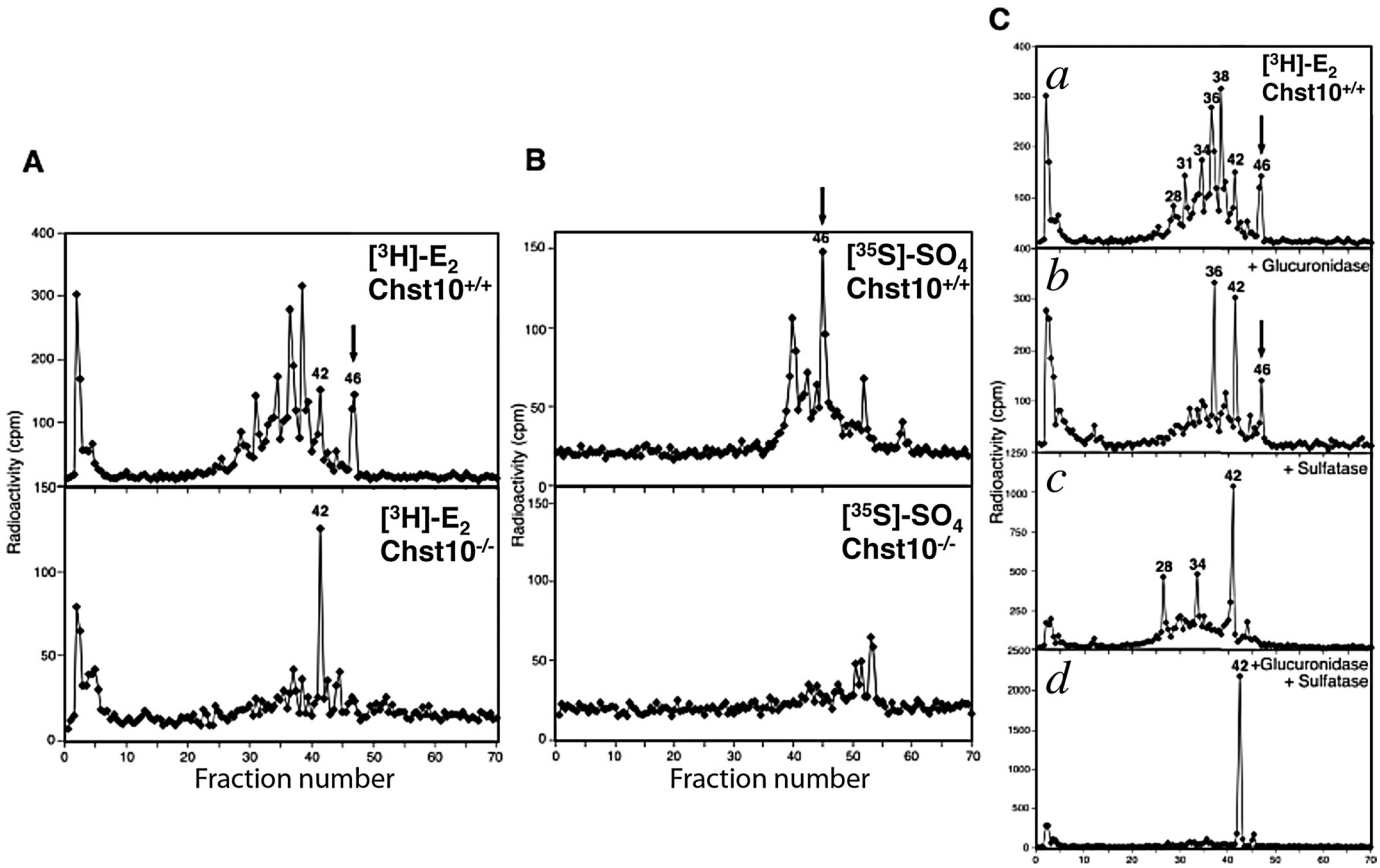

FIGURE 6. **Conversion of E2 *in vivo* in the mouse circulation.** *A,* [^{3}H]E_2 was injected intravenously into Chst10$^{+/+}$ (*upper panel*) or Chst10$^{-/-}$ (*lower panel*) female mice. [^{3}H]E_2 products were analyzed by HPLC using program 2 (see under "Materials and Methods"). Each peak at 42 and 46 min corresponds to E_2 and SO_3-GlcUA-E_2, respectively. *B,* [^{35}S]SO_4 was injected intravenously into Chst10$^{+/+}$ (*upper panel*) or Chst10$^{-/-}$ (*lower panel*) female mice. ^{35}S-Labeled products were analyzed by HPLC. *C,* digestion of [^{3}H]E_2 products by β-glucuronidase and arylsulfatase. *Panels a–d* show HPLC profiles of undigested [^{3}H]E_2 products (*panel a*), β-glucuronidase-digested products (*panel b*), arylsulfatase-digested products (*panel c*), and β-glucuronidase- and arylsulfatase-digested products (*panel d*). *Arrows* at 46 min depict SO_3-GlcUA-E_2.

tors of an ERE. These results strongly suggest that Chst10 down-regulates E_2 activity *in vivo*.

DISCUSSION

In this study, we report that Chst10, the enzyme responsible for biosynthesis of the carbohydrate antigen HNK-1, is capable of transferring sulfate to glucuronidated steroid hormones. This finding emerged from analysis of *Chst10*-deficient mice, which showed subfertility in both males and females. We hypothesized that Chst10 likely transfers sulfate to glucuronidated steroids, as the enzyme transfers sulfate to glucuronidated *N*-acetyl-lactosamines in glycoproteins and glycolipids (18, 33, 44, 56). Enzymatic activity of Chst10 to GlcUA steroids was confirmed by *in vitro* activity assays using structure-defined steroids as acceptor substrates (Fig. 3 and supplemental Fig. S4). Structures of products or sulfated steroid hormones were validated by mass spectrometry (Fig. 4 and supplemental Fig. S5). The biosynthesis of sulfated and glucuronidated steroid hormones in *Chst10*$^{+/+}$ but not in *Chst10*$^{-/-}$ mice was demonstrated using radioactive acceptor substrates or inorganic SO_3 intravenously injected into mice (Fig. 6). Glucuronyltransferases associated with ER membranes transfer GlcUA to various substrates, including steroids (50, 57). We speculate that steroids enter the luminal side of the ER, where they are

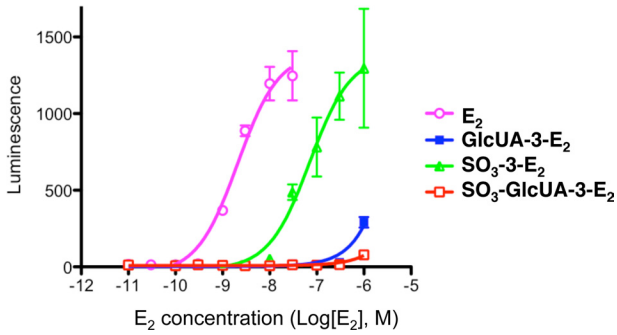

FIGURE 7. **ERE promoter assay using E_2, GlcUA-E_2, SO_3-3-E_2, and SO_3-GlcUA-E_2.** Luciferase activity was measured in HEK293T cells co-transfected with a gene encoding the ER plus an ERE-luciferase reporter gene and then treated with E_2, GlcUA-E_2, SO_3-3-E_2, or SO_3-GlcUA-E_2 at the indicated concentrations.

glucuronidated by glucuronyltransferase(s) and further sulfated by Chst10 in the Golgi.

Although the existence of SO_3-3-GlcUA-17-E_2 has been known (51), the structure of SO_3-GlcUA-3-E_2 presented here has not been reported previously. Because these two molecules are isomers and difficult to separate from each other (supplemental Fig. S6), they could have been missed by biochemical analysis such as mass spectrometry or HPLC. In this study, we hypothesized that GlcUA-3-E_2 is sulfated by Chst10 to produce

SO_3-GlcUA-3-E_2. Support for this hypothesis is shown in Figs. 3–6 and supplemental Fig. S6. Genetic deletion of *Chst10* reported here thus revealed a new structure, SO_3-GlcUA-3-E_2, which was heretofore unknown.

Glucuronidation of steroids is essential for maintaining hormonal balance and as a means to detoxify a wide variety of heterocyclic compounds. Glucuronidated steroids are easily transported around the body and are secreted into the urine. Sulfation of glucuronidated steroids may facilitate this process by promoting efficient elimination of products from the body into urine and feces, an activity suggested by the assay shown in supplemental Fig. S7. Loss of Chst10 in mutant mice apparently blocked down-regulation of steroids *in vivo*, resulting in up-regulation of hormonally active steroid hormones in female mice (Fig. 2). Steroid hormones are sulfated by Sult1E1 (45, 46). Sult1E1 null females (47, 48) exhibited phenotypes similar to those shown in this study of Chst10. In Sult1E1 null mice, the small litter size was attributed to a failure in placental development (47) and to ovulation defects resulting from a hormonal irregularity (48). Chst10 null mice also showed hormonal irregularities (supplemental Fig. S3). However, we have not determined the mechanism underlying the embryonic lethality seen in Chst10 nulls.

A mutant mouse line in which regions of the *Chst10* second exon were knocked out has been previously reported by others (58). These mice were viable and fertile, although the null mice showed impaired basal synaptic transmission and long term memory deficits. It is possible that our targeting construct (Fig. 1*A*) produced a fragment of Chst10 protein translated from exons 1–4, which may function as a dominant negative for other sulfotransferases and thus give rise to stronger phenotypes than previously reported *Chst10* null mice (58).

Chst10 is ubiquitously expressed in various tissues (44). Therefore, Chst10 protein may function in tissues other than reproductive organs. We observed that intravenously injected E_2 was not modified in *Chst10*$^{-/-}$ mice (Fig. 6), suggesting that activities of conjugation enzymes other than Chst10 are also suppressed in *Chst10* null mice. Future studies should define whether steroid-modifying enzymes interact with one another or are regulated together.

HNK-1 antigen is highly expressed in neuronal cells (Fig. 1*C*, supplemental Fig. S1*A*) (32, 33, 36). It is worth noting that sulfated steroids bind to vomeronasal receptors and function as pheromones in mice (59) and in fish (60). Pheromones are sex hormones, but their function is linked to the nervous systems. Expression of an SO_3-GlcUA-terminal structure as an HNK-1 antigen in neurons together with the existence of a similar structural modification of sex steroid hormones suggest that this modification may have an unidentified endocrine function linking steroid hormones to neuronal activation in mammals. Further studies are required to address this intriguing possibility.

Acknowledgments—We thank Drs. Xiakun Zhang and Lin Bingzhen of Sanford-Burnham Medical Research Institute for providing us with expression vectors for the estrogen receptor and Dr. Elise Lamar for editing the manuscript.

REFERENCES

1. Rosen, S. D. (2006) Homing in on L-selectin. *J. Immunol.* **177,** 3–4
2. Springer, T. A. (1994) Traffic signals for lymphocyte recirculation and leukocyte emigration. The multistep paradigm. *Cell* **76,** 301–314
3. McEver, R. P., Moore, K. L., and Cummings, R. D. (1995) Leukocyte trafficking mediated by selectin-carbohydrate interactions. *J. Biol. Chem.* **270,** 11025–11028
4. Butcher, E. C., and Picker, L. J. (1996) Lymphocyte homing and homeostasis. *Science* **272,** 60–66
5. Hirakawa, J., Tsuboi, K., Sato, K., Kobayashi, M., Watanabe, S., Takakura, A., Imai, Y., Ito, Y., Fukuda, M., and Kawashima, H. (2010) Novel anti-carbohydrate antibodies reveal the cooperative function of sulfated *N*- and *O*-glycans in lymphocyte homing. *J. Biol. Chem.* **285,** 40864–40878
6. Frenette, P. S., and Weiss, L. (2000) Sulfated glycans induce rapid hematopoietic progenitor cell mobilization: evidence for selectin-dependent and -independent mechanisms. *Blood* **96,** 2460–2468
7. McEver, R. P. (2002) Selectins. Lectins that initiate cell adhesion under flow. *Curr. Opin. Cell Biol.* **14,** 581–586
8. Yeh, J. C., Hiraoka, N., Petryniak, B., Nakayama, J., Ellies, L. G., Rabuka, D., Hindsgaul, O., Marth, J. D., Lowe, J. B., and Fukuda, M. (2001) Novel sulfated lymphocyte homing receptors and their control by a Core1 extension β1,3-*N*-acetylglucosaminyltransferase. *Cell* **105,** 957–969
9. Kawashima, H., Petryniak, B., Hiraoka, N., Mitoma, J., Huckaby, V., Nakayama, J., Uchimura, K., Kadomatsu, K., Muramatsu, T., Lowe, J. B., and Fukuda, M. (2005) *N*-Acetylglucosamine-6-*O*-sulfotransferases 1 and 2 cooperatively control lymphocyte homing through L-selectin ligand biosynthesis in high endothelial venules. *Nat. Immunol.* **6,** 1096–1104
10. Genbacev, O. D., Prakobphol, A., Foulk, R. A., Krtolica, A. R., Ilic, D., Singer, M. S., Yang, Z. Q., Kiessling, L. L., Rosen, S. D., and Fisher, S. J. (2003) Trophoblast L-selectin-mediated adhesion at the maternal-fetal interface. *Science* **299,** 405–408
11. Rosen, S. D. (2004) Ligands for L-selectin. Homing, inflammation, and beyond. *Annu. Rev. Immunol.* **22,** 129–156
12. Fukuda, M. N., and Sugihara, K. (2008) An integrated view of L-selectin and trophinin function in human embryo implantation. *J. Obstet. Gynaecol. Res.* **34,** 129–136
13. Rapraeger, A. C., Krufka, A., and Olwin, B. B. (1991) Requirement of heparan sulfate for bFGF-mediated fibroblast growth and myoblast differentiation. *Science* **252,** 1705–1708
14. Mi, Y., Fiete, D., and Baenziger, J. U. (2008) Ablation of GalNAc-4-sulfotransferase-1 enhances reproduction by altering the carbohydrate structures of luteinizing hormone in mice. *J. Clin. Invest.* **118,** 1815–1824
15. Akama, T. O., Nishida, K., Nakayama, J., Watanabe, H., Ozaki, K., Nakamura, T., Dota, A., Kawasaki, S., Inoue, Y., Maeda, N., Yamamoto, S., Fujiwara, T., Thonar, E. J., Shimomura, Y., Kinoshita, S., Tanigami, A., and Fukuda, M. N. (2000) Macular corneal dystrophy type I and type II are caused by distinct mutations in a new sulphotransferase gene. *Nat. Genet.* **26,** 237–241
16. Bullock, S. L., Fletcher, J. M., Beddington, R. S., and Wilson, V. A. (1998) Renal agenesis in mice homozygous for a gene trap mutation in the gene encoding heparan sulfate 2-sulfotransferase. *Genes Dev.* **12,** 1894–1906
17. Tsuda, M., Kamimura, K., Nakato, H., Archer, M., Staatz, W., Fox, B., Humphrey, M., Olson, S., Futch, T., Kaluza, V., Siegfried, E., Stam, L., and Selleck, S. B. (1999) The cell-surface proteoglycan Dally regulates Wingless signalling in *Drosophila*. *Nature* **400,** 276–280
18. Chou, D. K., Ilyas, A. A., Evans, J. E., Costello, C., Quarles, R. H., and Jungalwala, F. B. (1986) Structure of sulfated glucuronyl glycolipids in the nervous system reacting with HNK-1 antibody and some IgM paraproteins in neuropathy. *J. Biol. Chem.* **261,** 11717–11725
19. Hiraiwa, N., Fukuda, Y., Imura, H., Tadano-Aritomi, K., Nagai, K., Ishizuka, I., and Kannagi, R. (1990) Accumulation of highly acidic sulfated glycosphingolipids in human hepatocellular carcinoma defined

by a series of monoclonal antibodies. *Cancer Res.* **50,** 2917–2928
20. Loveless, R. W., Yuen, C. T., Tsuiji, H., Irimura, T., and Feizi, T. (1998) Monoclonal antibody 91.9H raised against sulfated mucins is specific for the 3′-sulfated Lewisa tetrasaccharide sequence. *Glycobiology* **8,** 1237–1242
21. Tsuji, Y., Fukuda, H., Iuchi, A., Ishizuka, I., and Isojima, S. (1992) Sperm immobilizing antibodies react to the 3-*O*-sulfated galactose residue of seminolipid on human sperm. *J. Reprod. Immunol.* **22,** 225-236
22. Yamakawa, N., Sato, C., Miyata, S., Maehashi, E., Toriyama, M., Sato, N., Furuhata, K., and Kitajima, K. (2007) Development of sensitive chemical and immunochemical methods for detecting sulfated sialic acids and their application to glycoconjugates from sea urchin sperm and eggs. *Biochimie* **89,** 1396–1408
23. Shibata, T. K., Matsumura, F., Wang, P., Yu, S., Chou, C. C., Khoo, K. H., Kitayama, K., Akama, T. O., Sugihara, K., Kanayama, N., Kojima-Aikawa, K., Seeberger, P. H., Fukuda, M., Suzuki, A., Aoki, D., and Fukuda, M. N. (2012) Identification of mono- and disulfated *N*-acetyl-lactosaminyl oligosaccharide structures as epitopes specifically recognized by humanized monoclonal antibody HMOCC-1 raised against ovarian cancer. *J. Biol. Chem.* **287,** 6592–6602
24. Abo, T., Cooper, M. D., and Balch, C. M. (1982) Postnatal expansion of the natural killer and killer cell population in humans identified by the monoclonal HNK-1 antibody. *J. Exp. Med.* **155,** 321–326
25. Abo, T., and Balch, C. M. (1981) A differentiation antigen of human NK and K cells identified by a monoclonal antibody (HNK-1). *J. Immunol.* **127,** 1024–1029
26. Schachner, M., and Martini, R. (1995) Glycans and the modulation of neural-recognition molecule function. *Trends Neurosci.* **18,** 183–191
27. Yanagisawa, M., Taga, T., Nakamura, K., Ariga, T., and Yu, R. K. (2005) Characterization of glycoconjugate antigens in mouse embryonic neural precursor cells. *J. Neurochem.* **95,** 1311–1320
28. Yuen, C. T., Chai, W., Loveless, R. W., Lawson, A. M., Margolis, R. U., and Feizi, T. (1997) Brain contains HNK-1 immunoreactive *O*-glycans of the sulfoglucuronyl lactosamine series that terminate in 2-linked or 2,6-linked hexose (mannose). *J. Biol. Chem.* **272,** 8924–8931
29. Ariga, T., Kohriyama, T., Freddo, L., Latov, N., Saito, M., Kon, K., Ando, S., Suzuki, M., Hemling, M. E., Rinehart, K. L., Jr., *et al.* (1987) Characterization of sulfated glucuronic acid containing glycolipids reacting with IgM M-proteins in patients with neuropathy. *J. Biol. Chem.* **262,** 848–853
30. Kleene, R., and Schachner, M. (2004) Glycans and neural cell interactions. *Nat. Rev. Neurosci.* **5,** 195–208
31. Fukui, S., Feizi, T., Galustian, C., Lawson, A. M., and Chai, W. (2002) Oligosaccharide microarrays for high-throughput detection and specificity assignments of carbohydrate-protein interactions. *Nat. Biotechnol.* **20,** 1011–1017
32. Kruse, J., Mailhammer, R., Wernecke, H., Faissner, A., Sommer, I., Goridis, C., and Schachner, M. (1984) Neural cell adhesion molecules and myelin-associated glycoprotein share a common carbohydrate moiety recognized by monoclonal antibodies L2 and HNK-1. *Nature* **311,** 153–155
33. Ong, E., Suzuki, M., Belot, F., Yeh, J. C., Franceschini, I., Angata, K., Hindsgaul, O., and Fukuda, M. (2002) Biosynthesis of HNK-1 glycans on *O*-linked oligosaccharides attached to the neural cell adhesion molecule (NCAM). The requirement for core 2 β1,6-*N*-acetylglucosaminyltransferase and the muscle-specific domain in NCAM. *J. Biol. Chem.* **277,** 18182–18190
34. McGarry, R. C., Helfand, S. L., Quarles, R. H., and Roder, J. C. (1983) Recognition of myelin-associated glycoprotein by the monoclonal antibody HNK-1. *Nature* **306,** 376–378
35. Kruse, J., Keilhauer, G., Faissner, A., Timpl, R., and Schachner, M. (1985) The J1 glycoprotein–a novel nervous system cell adhesion molecule of the L2/HNK-1 family. *Nature* **316,** 146–148
36. Suzuki-Anekoji, M., Suzuki, M., Kobayashi, T., Sato, Y., Nakayama, J., Suzuki, A., Bao, X., Angata, K., and Fukuda, M. (2011) HNK-1 glycan functions as a tumor suppressor for astrocytic tumor. *J. Biol. Chem.* **286,** 32824–32833
37. Morita, I., Kakuda, S., Takeuchi, Y., Itoh, S., Kawasaki, N., Kizuka, Y., Kawasaki, T., and Oka, S. (2009) HNK-1 glyco-epitope regulates the stability of the glutamate receptor subunit GluR2 on the neuronal cell surface. *J. Biol. Chem.* **284,** 30209–30217
38. Abbott, K. L., Matthews, R. T., and Pierce, M. (2008) Receptor tyrosine phosphatase β (RPTPβ) activity and signaling are attenuated by glycosylation and subsequent cell surface galectin-1 binding. *J. Biol. Chem.* **283,** 33026–33035
39. Bleckmann, C., Geyer, H., Lieberoth, A., Splittstoesser, F., Liu, Y., Feizi, T., Schachner, M., Kleene, R., Reinhold, V., and Geyer, R. (2009) *O*-Glycosylation pattern of CD24 from mouse brain. *Biol. Chem.* **390,** 627–645
40. Künemund, V., Jungalwala, F. B., Fischer, G., Chou, D. K., Keilhauer, G., and Schachner, M. (1988) The L2/HNK-1 carbohydrate of neural cell adhesion molecules is involved in cell interactions. *J. Cell Biol.* **106,** 213–223
41. McKeon, R. J., Schreiber, R. C., Rudge, J. S., and Silver, J. (1991) Reduction of neurite outgrowth in a model of glial scarring following CNS injury is correlated with the expression of inhibitory molecules on reactive astrocytes. *J. Neurosci.* **11,** 3398–3411
42. Terayama, K., Oka, S., Seiki, T., Miki, Y., Nakamura, A., Kozutsumi, Y., Takio, K., and Kawasaki, T. (1997) Cloning and functional expression of a novel glucuronyltransferase involved in the biosynthesis of the carbohydrate epitope HNK-1. *Proc. Natl. Acad. Sci. U.S.A.* **94,** 6093–6098
43. Bakker, H., Friedmann, I., Oka, S., Kawasaki, T., Nifant'ev, N., Schachner, M., and Mantei, N. (1997) Expression cloning of a cDNA encoding a sulfotransferase involved in the biosynthesis of the HNK-1 carbohydrate epitope. *J. Biol. Chem.* **272,** 29942–29946
44. Ong, E., Yeh, J. C., Ding, Y., Hindsgaul, O., and Fukuda, M. (1998) Expression cloning of a human sulfotransferase that directs the synthesis of the HNK-1 glycan on the neural cell adhesion molecule and glycolipids. *J. Biol. Chem.* **273,** 5190–5195
45. Ong, E., Yeh, J. C., Ding, Y., Hindsgaul, O., Pedersen, L. C., Negishi, M., and Fukuda, M. (1999) Structure and function of HNK-1 sulfotransferase. Identification of donor and acceptor binding sites by site-directed mutagenesis. *J. Biol. Chem.* **274,** 25608–25612
46. Pasqualini, J. R. (2009) Estrogen sulfotransferases in breast and endometrial cancers. *Ann. N.Y. Acad. Sci.* **1155,** 88–98
47. Tong, M. H., Jiang, H., Liu, P., Lawson, J. A., Brass, L. F., and Song, W. C. (2005) Spontaneous fetal loss caused by placental thrombosis in estrogen sulfotransferase-deficient mice. *Nat. Med.* **11,** 153–159
48. Gershon, E., Hourvitz, A., Reikhav, S., Maman, E., and Dekel, N. (2007) Low expression of COX-2, reduced cumulus expansion, and impaired ovulation in SULT1E1-deficient mice. *FASEB J.* **21,** 1893–1901
49. Simpson, E. R., and Davis, S. R. (2001) Minireview. Aromatase and the regulation of estrogen biosynthesis–some new perspectives. *Endocrinology* **142,** 4589–4594
50. Tukey, R. H., and Strassburg, C. P. (2000) Human UDP-glucuronosyltransferases. Metabolism, expression, and disease. *Annu. Rev. Pharmacol. Toxicol.* **40,** 581–616
51. Raftogianis, R., Creveling, C., Weinshilboum, R., and Weisz, J. (2000) Estrogen metabolism by conjugation. *J. Natl. Cancer Inst. Monogr.* **27,** 113–124
52. Caligioni, C. S. (2009) Assessing reproductive status/stages in mice. *Curr. Protoc. Neurosci.* **48,** A41.1–A41.8
53. Ghosh, R., Kamboj, V. P., and Singh, M. M. (2001) Interaction with antiimplantation and estrogen antagonistic activities of DL-ormeloxifene, a selective estrogen receptor modulator, by tetracycline in female Sprague-Dawley rats. *Contraception* **64,** 261–269
54. Angata, K., Huckaby, V., Ranscht, B., Terskikh, A., Marth, J. D., and Fukuda, M. (2007) Polysialic acid-directed migration and differentiation of neural precursors are essential for mouse brain development. *Mol. Cell. Biol.* **27,** 6659–6668
55. Jensen, E. V., and DeSombre, E. R. (1973) Estrogen-receptor interaction. *Science* **182,** 126–134
56. Ilyas, A. A., Quarles, R. H., and Brady, R. O. (1984) The monoclonal antibody HNK-1 reacts with a human peripheral nerve ganglioside. *Biochem.*

Biophys. Res. Commun. **122,** 1206–1211
57. Fisher, M. B., Campanale, K., Ackermann, B. L., VandenBranden, M., and Wrighton, S. A. (2000) *In vitro* glucuronidation using human liver microsomes and the pore-forming peptide alamethicin. *Drug Metab. Dispos.* **28,** 560–566
58. Senn, C., Kutsche, M., Saghatelyan, A., Bösl, M. R., Löhler, J., Bartsch, U., Morellini, F., and Schachner, M. (2002) Mice deficient for the HNK-1 sulfotransferase show alterations in synaptic efficacy and spatial learning and memory. *Mol. Cell. Neurosci.* **20,** 712–729
59. Isogai, Y., Si, S., Pont-Lezica, L., Tan, T., Kapoor, V., Murthy, V. N., and Dulac, C. (2011) Molecular organization of vomeronasal chemoreception. *Nature* **478,** 241–245
60. Sorensen, P. W., Fine, J. M., Dvornikovs, V., Jeffrey, C. S., Shao, F., Wang, J., Vrieze, L. A., Anderson, K. R., and Hoye, T. R. (2005) Mixture of new sulfated steroids functions as a migratory pheromone in the sea lamprey. *Nat. Chem. Biol.* **1,** 324–328